Chinese Chemical Letters 35 (2024) 108903

Contents lists available at ScienceDirect

Chinese Chemical Letters

journal homepage: www.elsevier.com/locate/cclet

A nonradical oxidation process initiated by Ti-peroxo complex showed high specificity toward the degradation of tetracycline antibiotics

Jian Peng[a,b,1], Yue Jiang[a,b,1], Shuangyu Wu[a,b], Yanran Cheng[a,b], Jingyu Liang[a,b], Yixin Wang[a,b], Zhuo Li[b], Sijie Lin[a,b,*]

[a] College of Environmental Science and Engineering, Biomedical Multidisciplinary Innovation Research Institute, Shanghai East Hospital, Tongji University, Shanghai 200092, China

[b] Key Laboratory of Yangtze River Water Environment, Shanghai Institute of Pollution Control and Ecological Security, Tongji University, Shanghai 200092, China

ARTICLE INFO

Article history:
Received 22 April 2023
Revised 17 July 2023
Accepted 6 August 2023
Available online 9 August 2023

Keywords:
Nonradical oxidation
Metal-organic frameworks
Advanced oxidation process
Ti-peroxo complex
Antibiotics degradation

ABSTRACT

Nonradical oxidation has received wide attention in advanced oxidation processes for environmental remediation. Understanding the relationship between material characteristics and their ability to initiate nonradical oxidation processes is the key to better material design and performance. Herein, a novel titanium-based metal-organic framework MIL-125-Ti/H_2O_2 system was established to show a highly selective degradation efficacy toward tetracycline antibiotics. MIL-125-Ti with the abundance of TiO_6 octahedra units was found to effectively activate H_2O_2 under dark conditions by forming an oxidative Ti-peroxo complex. The presence of the Ti-peroxo complex, confirmed by UV-visible spectrophotometer, fourier transform infrared spectroscopy, and X-ray photoelectron spectroscopy characterizations, showed superior degradation (>95% removal rate) of oxytetracycline hydrochloride (OTC), doxycycline hydrochloride, chlortetracycline hydrochloride, and tetracycline. Density functional theory calculations were performed to assist the elucidation on the mechanism of H_2O_2 activation and antibiotics degradation. The MIL-125-Ti/H_2O_2 system was highly resistant to halogens and background organics, and could well maintain its original catalytic activity in actual water matrices. It retained the ability to degrade 75% of OTC within ten test cycles. This study provides new insight into the nonradical oxidation process initiated by the unique Ti-peroxo complex of Ti-based MOF.

Both radical and nonradical-based advanced oxidation processes (AOPs) possess unique advantages in removing toxic and recalcitrant organic pollutants. Reactive oxygen species (ROS) produced in typical radical-based AOPs, such as hydroxyl radicals (•OH), sulfate radicals ($SO_4^{\bullet-}$), and superoxide anion radicals ($^{\bullet}O_2^-$), play an important role in organic pollutants degradation [1,2]. However, these processes are challenged by interfering factors, including the varying pH, the background organics, and inorganics [3,4]. In this regard, the nonradical oxidation pathways have shown clear advantages, especially in complex environments where radical-quenching species are ubiquitous [5,6].

Although transition metal-based catalysts have been a focus to achieve nonradical oxidation, some of them (*e.g.*, Co_3O_4, CuO, ZnO) might cause unwanted hazardous effects due to the heavy metal content or experience compromised catalytic performance caused by the hydrolysis of metal ions (such as Fe^{3+}) within the catalyst [7–9]. In contrast, titanium-based catalysts have clear advantages of excellent biocompatibility and abundant natural reserves [2,10]. Previously, hollow TS-1 zeolites in combination with H_2O_2 were explored in organic synthesis for selective oxidation reaction processes [11]. It was intriguing to see that the Ti(IV) center reacted with H_2O_2 to form active intermediates, *i.e.* Ti-peroxo complexes (Ti-O-O-H) and these Ti-peroxo complexes exhibited strong oxidation abilities [12,13]. Such a nonradical oxidation pathway initiated by Ti-peroxo complexes could result in a novel degradation strategy toward organic pollutants.

The typical titanium-based catalysts contain a variety of Ti species, including TiO_4 species [14,15], TiO_5 species [16], TiO_6 species [17–19], and anatase [20]. Generally, Ti species with higher coordination states have higher oxidation ability. The higher activity of TiO_6 species compared to TiO_4 species is mainly due to the lower steric hindrance of their Ti-peroxo transition state,

* Corresponding author at: Key Laboratory of Yangtze River Water Environment, Shanghai Institute of Pollution Control and Ecological Security, Tongji University, Shanghai 200092, China.
E-mail address: lin.sijie@tongji.edu.cn (S. Lin).
[1] These authors contributed equally to this work.

https://doi.org/10.1016/j.cclet.2023.108903
1001-8417/

which makes it more favorable for catalyzing the oxidation process [17,21,22]. However, the presence of multiple titanium species would limit the effectiveness of their catalytic performance [23]. In addition, the ability of the Ti-peroxo complexes formed by the interaction with H_2O_2 and the quantity of Ti metal sites were two other factors determining the efficiency of the catalytic oxidation reaction [24]. Thus, it is reasonable to speculate that a titanium-based catalyst with as many TiO_6 species as possible and a high content of titanium metal sites would exert excellent catalytic activities.

A metal-organic framework (MOF) known as MIL-125-Ti is composed of Ti and terephthalic acid, where Ti exists in the form of hexa-liganded $TiO_5(OH)$ (MIL stands for Material from Institut Lavoisier) [25]. In addition, MIL-125-Ti has typical characteristics of metal-organic frameworks, including pore properties, high surface area, a significant content of metal sites (usually well-defined clusters), and spatially homogeneous distribution [26]. MIL-125-Ti was previously shown to catalyze H_2O_2 to achieve selective oxidation of alkylphenols due to the existence of well-defined titanium oxo-hydroxo clusters [27]. It was suggested that the reaction of H_2O_2 and MIL-125-Ti occurred on the surface of the catalyst rather than in the solution [28]. These studies revealed that the reaction between MIL-125-Ti and H_2O_2 could generate interfacial oxidative species, but the catalytic behavior and mechanism characteristics in aqueous phase conditions warrant further investigations.

Against this background, we set out to explore the formation and oxidation capacity of Ti-peroxo complexes in a MIL-125-Ti/H_2O_2 system. The Ti-peroxo complexes formed by MIL-125-Ti after reacting with H_2O_2 were characterized by UV-vis, FT-IR, and XPS. The degradation of the antibiotic oxytetracycline hydrochloride (OTC) was used to measure the oxidative capacity of the generated Ti-peroxo complexes. The non-radical mechanism for the generation of the Ti-peroxo complexes was verified by scavenging and EPR characterizations. Different anions concentrations, pH levels, and organic matter concentrations were considered while examining the impact on antibiotic removal. Furthermore, the system was tested for its effectiveness and selectiveness toward other tetracycline antibiotics, including tetracycline, chlortetracycline hydrochloride, and doxycycline hydrochloride.

The reagents, material preparation, and experimental procedures were described in Texts S1-S8 (Supporting information). The XRD pattern of the synthesized MIL-125-Ti confirmed that MIL-125-Ti was successfully prepared with a 3D reticular analogue of the $TiO_5(OH)$ structure (Fig. 1a) [25]. The XRD peak at 13.5°, classified as a (202) crystallographic plane, was one of the features of MIL-125-Ti with {001} facets. The representative SEM images showed that MIL-125-Ti exhibited a truncated octahedral morphology with co-exposed {001} and {111} crystal faces (Fig. 1b) [29]. Nitrogen adsorption-desorption experiments were used to examine the specific surface area and pore size distribution of MIL-125-Ti. As shown in Figs. 1c and d, the BET surface area of MIL-125-Ti was 1414.88 m^2/g and the average pore size (calculated by the BJH method) was 4.62 nm. The isotherm distribution showed a hysteresis loop isotherm with no obvious saturation plateau, with microporous and mesoporous characteristics.

Prior to the reaction with H_2O_2, MIL-125-Ti displayed a shoulder band at 275-300 nm in its UV-vis diffuse reflectance spectra (Fig. 1e), which corresponded to the O $2p \rightarrow$ Ti 3d charge transition in the Ti octahedral unit [30]. Another band centered at 230 nm was attributed to the π-π^* transition of the terephthalic acid (BDC) ligand. After reacting with H_2O_2, the powder form of MIL-125-Ti showed a clear color change, from white to yellow (Fig. 1e, inset). In the absorbance spectra, additional distinct absorption profiles were observed in the range of 370-500 nm, suggesting the presence of an O-O fraction in the Ti^{4+} center, an indicator of the presence of the Ti-peroxo complexes (Ti-OOH) [31,32].

FT-IR spectroscopy was used to confirm the differences between the functional groups on the surface of MIL-125-Ti before and after reacting with H_2O_2 (Fig. 1f). The peaks at 1587 cm^{-1}, 1536 cm^{-1}, and 1407 cm^{-1} were skeletal vibrations of the benzene ring. These peaks produced varying degrees of shift, resulting from the coordination of functional groups such as carboxylates on the benzene ring backbone to the Ti-oxo clusters in the metal-organic framework [33]. The band in the 400–800 cm^{-1} region was assigned to the O-Ti-O stretching vibration peak of the [TiO_6] ligand [25,34]. The absorption peak at 751 cm^{-1} was assigned as Ti-O stretching, which exhibited three small absorption peaks after the H_2O_2 treatment. These three absorption peaks mainly resulted from the difference in coordination between Ti-O and hydroxyl groups [35]. The peaks at 781 cm^{-1} and 738 cm^{-1} were assigned to the coordination of the hydroxyl group to Ti^{4+} (OH-Ti-O) and the double coordination protonation of O^{2-} (-OH-O-Ti), respectively. In the Raman spectrum of the MIL-125-Ti/H_2O_2 system (Fig. S1 in Supporting information), an enhanced vibrational mode at 632 cm^{-1} was observed, which corresponds to the presence of Ti-peroxide species, consistent with the conclusions drawn from the FT-IR [36]. More information could be found in Text S9 (Supporting information).

The XPS survey spectrum of MIL-125-Ti before and after reacting with H_2O_2 (Fig. S2a in Supporting information) suggested that the samples only contain Ti, O, and C elements. For the C 1s spectrum of MIL-125-Ti (Fig. S2b in Supporting information), the peaks at 284.80, 286.58, and 288.72 eV were attributed to C-C, C-O, and -C=O in carboxylic acid, respectively [34,37]. The O 1s spectrum of the MIL-125-Ti consisted of a peak at 531.77 eV and a shoulder at 530.16 eV (Fig. 1g), and these binding energy values corresponded to Ti-O in the Ti-O_x cluster and the carboxylate C=O in terephthalic acid. Upon H_2O_2 reaction, an extra peak at 533.16 eV was found to fit the left tail at around 533-536 eV, and this peak could be assigned to the Ti-peroxo complexes [38,39]. In the Ti 2p spectrum (Fig. 1h), the two peaks at 458.75 and 464.45 eV were assigned to Ti $2p_{3/2}$ and Ti $2p_{1/2}$, indicating that the Ti in the Ti-O_x cluster maintains the oxidation state IV [26]. Upon H_2O_2 reaction, the binding energy of Ti $2p_{3/2}$ decreased from 458.75 eV to 458.66 eV, indicating that the chemical environment of Ti^{4+} changed with electropositivity enhancement around them [15,23]. Based on the above analysis, it could be seen that MIL-125-Ti with a pure [TiO_6] structure produced Ti-peroxo complexes upon reacting with H_2O_2. The formation of such complexes altered the chemical environment around the Ti species to give it an oxidizing capability.

Typical antibiotic OTC was selected to determine the oxidizing and degradation ability of the Ti-peroxo complexes produced by MIL-125-Ti upon reacting with H_2O_2. Before degradation experiments, adsorption experiments were performed to investigate the adsorption-desorption equilibrium. In a 50 mg/L OTC solution, MIL-125-Ti could adsorb more than 50% of OTC and the adsorption-desorption equilibrium of OTC molecules was reached at 180 min (Fig. S3 in Supporting information). The adsorption kinetic and thermodynamic analysis showed that the adsorption of OTC on MIL-125-Ti tended to be influenced by chemisorption and readily adsorbed on the catalyst surface, which provides a basis for interfacial oxidation (Text S10, Figs. S4 and S5 in Supporting information). The OTC started to decompose when the MIL-125-Ti system was dosed with H_2O_2, resulting in the removal of 96% of the OTC from the solution within 180 min (Fig. S6 in Supporting information). It indicated that the reaction between MIL-125-Ti and H_2O_2 produced oxidizing substances that caused the degradation of OTC. But it remained to be answered whether it is due to the presence of Ti-peroxo complexes.

To determine whether the MIL-125-Ti/H_2O_2 system degraded the OTC through the generation of radicals, EPR analyses, and radical scavenging tests were performed, and the results were shown

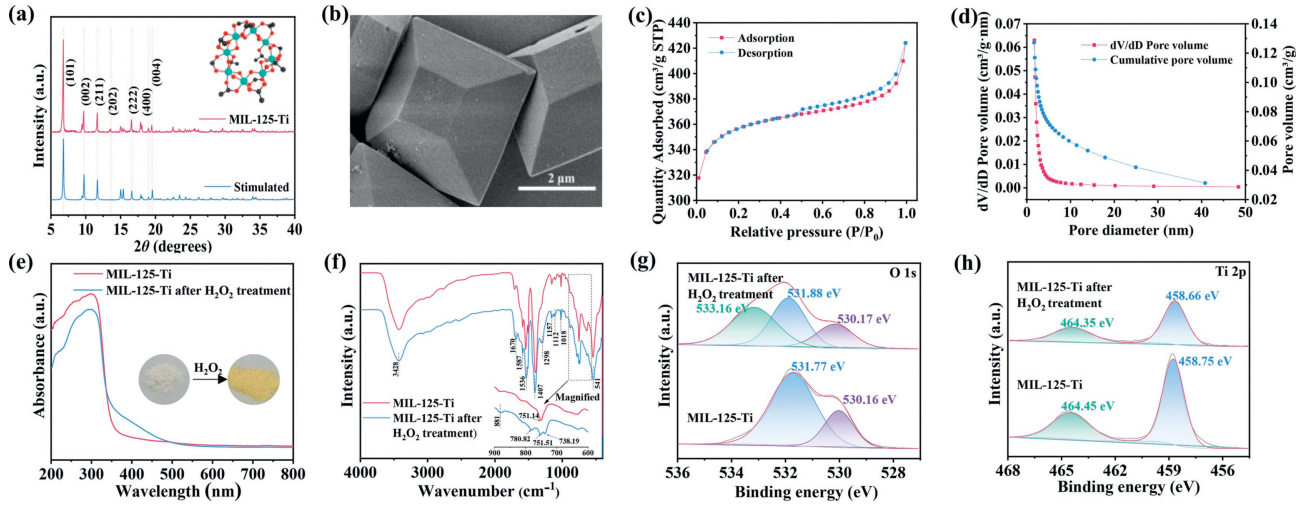

Fig. 1. Structural and characterizations of MIL-125-Ti catalyst. (a) XRD patterns. (b) SEM image of MIL-125-Ti. (c) N_2 adsorption-desorption isotherm and (d) pore size distribution of MIL-125-Ti. (e) UV-vis and (f) FT-IR spectra of MIL-125-Ti before and after treated with H_2O_2. XPS spectra of MIL-125-Ti before and after treated with H_2O_2: (g) O 1s, (h) Ti 2p. The secondary building unit of MIL-125-Ti is shown in the upper right corner of Fig. 1a with the first carbon atom from the benzene rings of MIL-125-Ti shown in black. Titanium and oxygen atoms are shown in cyan and red, respectively.

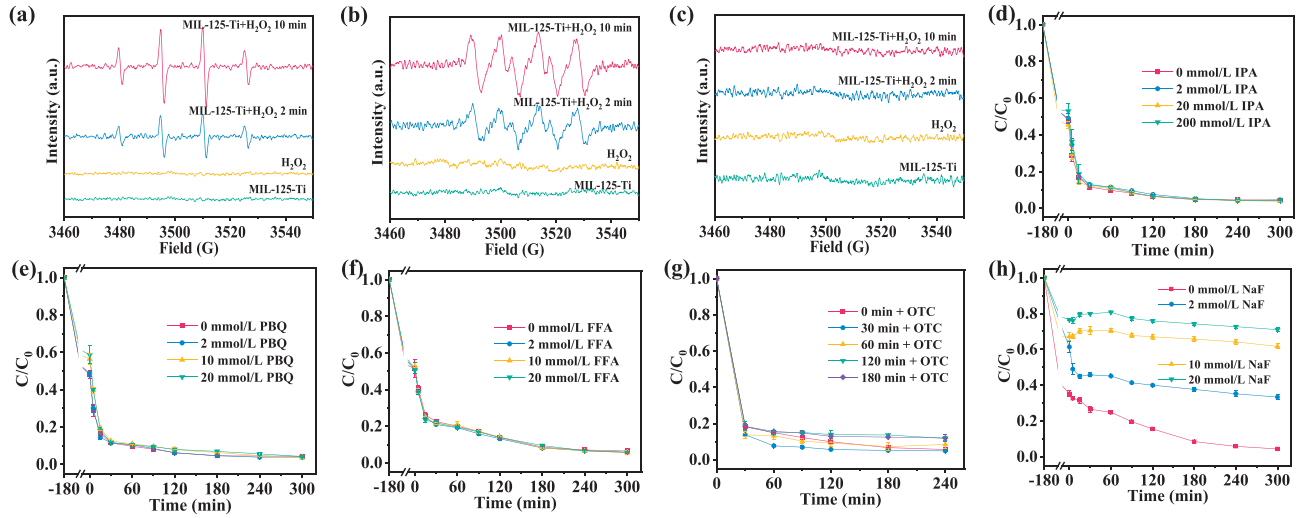

Fig. 2. Identification of the ROS in MIL-125-Ti/H_2O_2 system. EPR spectra of (a, b) DMPO and (c) TEMP in MIL-125-Ti/H_2O_2 system. Effects of different concentrations of radical scavengers (d) IPA, (e) PBQ, and (f) FFA on the degradation of OTC in MIL-125-Ti/H_2O_2. (g) The removal efficiency of OTC under different regular time intervals for pollutant adding after mixing MIL-125-Ti with H_2O_2. (h) Effect of different concentrations of NaF in MIL-125-Ti/ H_2O_2 system for OTC degradation. Conditions: [OTC] = 50 mg/L, [H_2O_2] = 2 mmol/L, [MIL-125-Ti] = 0.3 g/L.

in Figs. 2a and b. No distinctive signals of DMPO-$^{\bullet}$OH were detected in MIL-125-Ti alone as well as in H_2O_2 under dark conditions. A 1:2:2:1 hyperfine splitting signal belonging to DMPO-$^{\bullet}$OH and a weaker 1:1:1:1 hyperfine splitting signal belonging to DMPO-$^{\bullet}O_2^-$ were detected in the MIL-125-Ti/H_2O_2 system, indicating that only small amount of $^{\bullet}$OH and $^{\bullet}O_2^-$ were produced in the system. Additionally, no oxygen vacancies ($g = 2.003$), as well as Ti^{3+} ($g \approx 1.94$) signals, were observed in MIL-125-Ti (Fig. S7 in Supporting information), which indicated that the material had no surface oxygen vacancies and there was no Ti^{3+} involved in the catalytic process [39]. Moreover, TEMP was used as a $^1O_2$ trap to produce TEMPO with a distinct three-line hyperfine splitting signal. No obvious signal was found in the MIL-125-Ti/H_2O_2 system (Fig. 2c). Therefore, $^1O_2$ was not the major ROS in this system either.

Radical scavenging experiments were also conducted in the MIL-125-Ti/H_2O_2 system to determine the major ROS involved in OTC degradation and their contribution to OTC degradation. As shown in Figs. 2d-f, the degradation of OTC by the MIL-125-Ti/H_2O_2 system was not inhibited in the presence of different concentrations of IPA, PBQ, or FFA. These results further strengthened the argument that $^{\bullet}$OH, $^{\bullet}O_2^-$ and $^1O_2$ did not play a major role in the degradation and nonradical pathways might be the main factor in the MIL-125-Ti/H_2O_2 system. To demonstrate the MIL-125-Ti/H_2O_2 degraded OTC through the nonradical pathway, the presence of surface-bound radicals was determined by pre-mixing MIL-125-Ti and H_2O_2 followed by delayed addition of OTC at different time intervals. The decrease in the removal rate of OTC was minimum indicating that the short-lifetime radicals were not likely the reason for OTC degradation (Fig. 2g). Also, the addition of F^- significantly reduced the removal rate of OTC (Fig. 2h). This could be mainly due to the occupation of the adsorption sites of the MIL-125-Ti by the fluorine hydrogen bonds [40], which severely inhibits the generation of surface-complexed reactive substances and the surface adsorption with OTC. Meanwhile, the fact that the removal efficiency of OTC did not improve indicates that surface-

bound radicals did not participate in the degradation of OTC. This is supported by the observation that the addition of F^- significantly increased the solution-$^{\bullet}OH$ content by promoting the release of surface-bound radicals, leading to enhanced degradation [41,42]. These results confirmed that the catalytic oxidation of OTC by the MIL-125-Ti/H_2O_2 system was initiated by the surface complexation and the presence of Ti-peroxo complexes. Together, the degradation of OTC in the MIL-125-Ti/H_2O_2 system was achieved through a nonradical pathway based on the surface-complexed reactive substances, *i.e.* the Ti-peroxo complexes.

To further evaluate the catalytic performance of the MIL-125-Ti/H_2O_2 system, the influence of operating parameters on OTC degradation was evaluated. The effect of H_2O_2 dosage on the OTC degradation showed that the increase of H_2O_2 concentration (0.2-2.0 mmol/L) increased the removal of OTC from 66.0% to 91.3% at 60 min (Fig. S8 in Supporting information). However, no increase in the removal rate of OTC was observed with the H_2O_2 concentration beyond 2 mmol/L. Additionally, it was noteworthy that the MIL-125-Ti/H_2O_2 system was also able to remove more than 83% of OTC at 100 mg/L (Fig. S9 in Supporting information). There were no differences in the rate of OTC removal at various pH (3.5-11), suggesting that the change in pH has little effect on the MIL-125-Ti/H_2O_2 system (Fig. S10 in Supporting information). This also confirmed that the MIL-125-Ti/H_2O_2 system was likely operating on a nonradical pathway [40,43].

Anions and organic matter (such as NaHA) are commonly found in actual water environments, which may affect the performance of the MIL-125-Ti/H_2O_2 system. As shown in Figs. S11a-e (Supporting information), the effect of all the anions was minimal, except for the presence of 10 mmol/L $H_2PO_4^-$ which significantly affected the removal of OTC. This was likely due to the excess of $H_2PO_4^-$ might occupy the adsorption site of MIL-125-Ti, similar to the effect of F^- [31,44]. In the presence of NaHA at a wide concentration range (10-100 mg/L), OTC removal was largely unaffected (Fig. S11f in Supporting information), suggesting this nonradical-dominated system had better resistance to interference from natural organic matter. Additionally, compared to ultrapure water, the MIL-125-Ti/H_2O_2 system exhibited similar OTC removal efficiency in other water matrices (Fig. S12 in Supporting information). The exceptional resistance to interference in complex water matrices further demonstrated the superior performance of the MIL-125-Ti/H_2O_2 system for the removal of contaminants from contaminated practical water. The MIL-125-Ti/H_2O_2 system was compared to other previously reported H_2O_2 systems (Table S6 in Supporting information) and it demonstrated comparable efficacy in removing tetracycline antibiotics with lower amount of H_2O_2 consumed. Furthermore, the MIL-125-Ti maintained relatively stable catalytic performance in OTC removal without any regeneration process and was able to remove more than 75% of OTC after 10 reuses (Fig. S13 in Supporting information). There were only trace amounts of titanium leached as determined in the filtrate by ICP-OES. Neither the MIL-125-Ti nor the solution after degradation of OTC had any significant effects on the survival and hatching rates of zebrafish embryos (Fig. S14 in Supporting information). The XRD patterns of the fresh and used MIL-125-Ti were not significantly different, but the used MIL-125-Ti showed a collapse of the structure (Figs. S15 and S16 in Supporting information).

To investigate whether the MIL-125-Ti/H_2O_2 system has selectivity and specificity toward a certain type of organic pollutants, tetracycline antibiotics including oxytetracycline hydrochloride (OTC), tetracycline (TC), chlortetracycline hydrochloride (CTC), doxycycline hydrochloride (DOC) were tested. The MIL-125-Ti/H_2O_2 system was effective in the removal of all tetracycline antibiotics, with 94.7% degradation of TC, 89.2% degradation of CTC, and 98.5% degradation of DOC (Fig. S17a in Supporting information). The selectivity of the MIL-125-Ti/H_2O_2 system for the degradation of tetracycline antibiotics was verified by comparing the degradation of OTC and TC with three additional contaminants, *i.e.* sulfamethoxazole (SMX), acetaminophen (AAP), and bisphenol A (BPA). As shown in Fig. S17b (Supporting information), only the tetracycline antibiotics were removed by more than 94%. In contrast, SMX and AAP were only removed by 26.3% and 33.9%, respectively, while BPA was removed by only 12.2%. Such specificity was likely due to the interfacial properties of this nonradical system, where efficient degradation would not occur if the contaminant had a low adsorption tendency on the material surface to interact with the Ti-peroxo complexes.

The degradation intermediates of OTC in the MIL-125-Ti/H_2O_2 system were identified by UPLC-TOF. The information related to the detected degradation intermediates of OTC is listed in Table S7 and Figs. S18-S21 (Supporting information). Based on the analysis of mass spectra, a potential OTC degradation pathway was suggested (Text S11 and Fig. S22 in Supporting information).

To further understand the activation of H_2O_2 by MIL-125-Ti, the catalytic process of MIL-125-Ti was calculated using DFT. With a favorable reaction energy ΔE of -8.217 kcal/mol, the MIL-125-Ti-H_2O_2 species may give rise to two configurations, MIL-125-Ti-O1 (configuration I) and MIL-125-Ti-O2 (configuration II) (Fig. 3a). The energy for the formation of configuration II from MIL-125-Ti-H_2O_2 (ΔE = -0.788 kcal/mol) was lower than that for the formation of configuration I (ΔE =3.988 kcal/mol). Therefore, the configuration II was used for subsequent calculations.

Upon addition, OTC molecules interacted with the Ti-OH-Ti and Ti-O-Ti sites within the configuration II pore channel through multiple hydrogen bonding, resulting in a very strong physical adsorption with an adsorption energy of 54.010 kcal/mol. The physical adsorption was consistent with the experimental results. In addition, four sites on the OTC with double bonds (sites 1, 2, 3, and 4) were selected as Ti-peroxo complexes attack regions for the simulations (Fig. 3b), where the sites 2, 3, 4 were common attack sites for free radicals [45,46]. The step of OTC-O1 obtained from Ti-peroxo complex attacked site 1 of configuration II (ΔE = −52.237 kcal/mol)

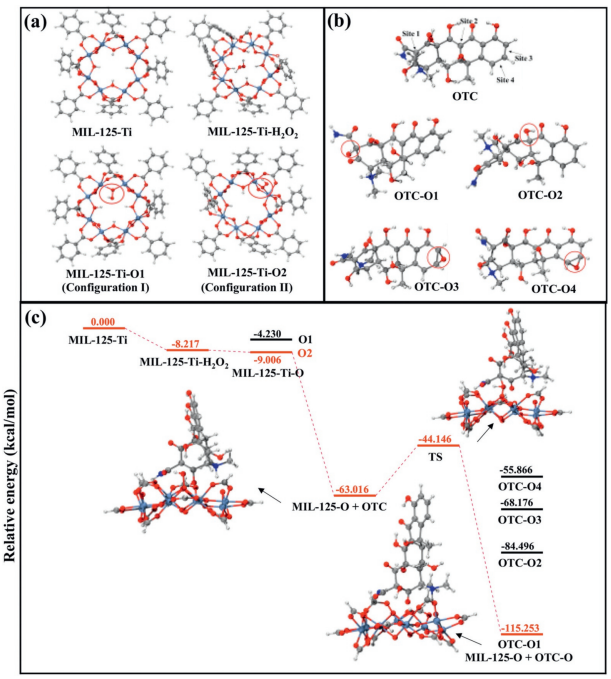

Fig. 3. DFT calculations. (a) Different configurations resulting from H_2O_2 activation by MIL-125-Ti. (b) Different sites of OTC were attacked by Ti-peroxo complex. (c) Calculated energy surface of H_2O_2 activation on MIL-125-Ti with OTC oxidation. Atomic colors: Ti (bice), C (gray), N (blue), O (red), H (white).

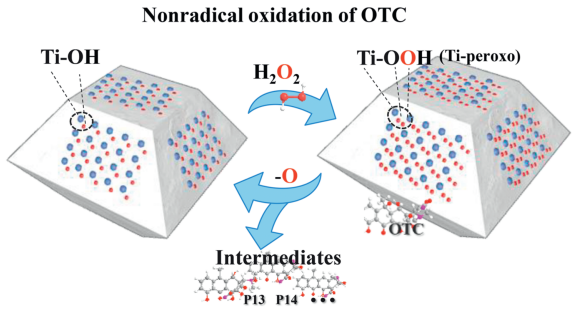

Fig. 4. Schematic illustration of activation mechanism in MIL-125-Ti/H_2O_2 system.

was much easier than that of OTC-O2, OTC-O3 and OTC-O4 obtained from attack sites 2, 3 and 4 (Fig. 3c). The transition state of this step of the primitive reaction was then further calculated and the transition state energy barrier was obtained as 18.870 kcal/mol, indicating that the reaction can be carried out at room temperature. Upon completion of oxygen transfer to the OTC, configuration II reverted to the MIL-125-Ti by solvent-mediated proton transfer and was ready for cyclic catalysis. This accessible transition state may be considerably lower in the proton medium due to the ease of solvent-mediated proton transfer [47].

Based on this study and previous reports [31,38,44], a possible mechanism for OTC degradation in the H_2O_2 activation system catalyzed by MIL-125-Ti was proposed (Fig. 4). First, H_2O_2 formed intermediate titanium hydroperoxides (Ti-O-O-H) with the Ti(IV) center of MIL-125-Ti, and this structure could react with the OTC adsorbed on the surface of MIL-125-Ti. The OTC was oxidized, and the Ti-OOH structure was converted back to the Ti-OH structure. Therefore, this was a typical nonradical oxidation process for OTC degradation.

In conclusion, this study demonstrated an effective nonradical oxidation pathway for the degradation of tetracycline antibiotics by a MIL-125-Ti/H_2O_2 system. The nonradical oxidation was initiated by the Ti-peroxo complexes formed after the reaction of MIL-125-Ti with H_2O_2. Both the radical quenching experiments and EPR analysis confirmed that the degradation of OTC was dominated by a nonradical oxidation process. In addition, this system could proceed in a wide pH range and practical water matrices, while demonstrating good resistance to conventional radical scavengers, halogens, and background organic substances. The pathway of OTC degradation was also postulated and the degradation efficiency was maintained above 75% removal rate after 10 test cycles. DFT calculations confirmed the reaction of MIL-125-Ti and H_2O_2 could produce a unique Ti-peroxo complexes structure that was thermodynamically favorable and the oxidation of OTC by this structure was feasible. The formation of Ti-peroxo complexes was the key to the high selectivity of the MIL-125-Ti/H_2O_2 system toward the degradation of tetracycline antibiotics.

Declaration of competing interest

The authors declare that they have no known competing financial interests or personal relationships that could have appeared to influence the work reported in this paper.

Acknowledgments

This work was supported by the National Natural Science Foundation of China (Nos. 21777116, 22176150) and the Fundamental Research Funds for the Central Universities.

Supplementary materials

Supplementary material associated with this article can be found, in the online version, at doi:10.1016/j.cclet.2023.108903.

References

[1] F. Gozzo, J. Mol. Catal. A: Chem. 171 (2001) 1–22.
[2] Y. Jiang, D. Baimanov, S. Jin, et al., Proc. Natl. Acad. Sci. U. S. A. 120 (2023) e2210211120.
[3] F.J. Rivas, F.J. Beltran, J. Frades, et al., Water Res. 35 (2001) 387–396.
[4] P.H. Shao, J.Y. Tian, F. Yang, et al., Adv. Funct. Mater. 28 (2018) 1705295.
[5] S.J. Ye, G.M. Zeng, X.F. Tan, et al., Appl. Catal. B: Environ. 269 (2020) 118850.
[6] J.B. Chen, J. Xu, T.C. Liu, et al., J. Hazard. Mater. 386 (2020) 121656.
[7] M.M. Wang, Y.K. Cui, H.Y. Cao, et al., Appl. Catal. B: Environ. 282 (2021) 119585.
[8] T. Zhang, Y. Chen, Y.R. Wang, et al., Environ. Sci. Technol. 48 (2014) 5868–5875.
[9] Y. Bao, C. Lian, K. Huang, et al., Angew. Chem. Int. Ed. 61 (2022) e2022095.
[10] J. Song, Z. Huang, J. Mao, et al., Chem. Eng. J. 396 (2020) 125246.
[11] M. Lin, C.J. Xia, B. Zhu, et al., Chem. Eng. J. 295 (2016) 370–375.
[12] M.G. Zuo, X.Q. Huang, J.X. Li, et al., Catal. Sci. Technol. 9 (2019) 2923–2930.
[13] X. Feng, D. Lin, D. Chen, et al., Sci. Bull. 66 (2021) 1945–1949.
[14] L. Xu, J.H. Ding, Y.L. Yang, et al., J. Catal. 309 (2014) 1–10.
[15] Y. Wei, G. Li, R.M. Su, et al., Appl. Catal. A: Gen. 582 (2019) 117108.
[16] Y. Zuo, M. Liu, T. Zhang, et al., RSC Adv. 5 (2015) 17897–17904.
[17] Y.Y. Wang, L. Li, R.S. Bai, et al., Chin. J. Catal. 42 (2021) 2189–2196.
[18] Q. Guo, K.J. Sun, Z.C. Feng, et al., Chem. Eur. J. 18 (2012) 13854–13860.
[19] W.J. Xu, T.J. Zhang, R.S. Bai, et al., J. Mater. Chem. A 8 (2020) 9677–9683.
[20] L.D. Sanchez, S. Taxt-Lamolle, E.O. Hole, et al., Appl. Catal. B: Environ. 142 (2013) 662–667.
[21] L.Z. Wu, X.J. Deng, S.F. Zhao, et al., Chem. Commun. 52 (2016) 8679–8682.
[22] J.P. Yin, H. Xu, B.W. Wang, et al., Catal. Sci. Technol. 10 (2020) 6050–6064.
[23] L. Xu, D.D. Huang, C.G. Li, et al., Chem. Commun. 51 (2015) 9010–9013.
[24] W.J. Zhou, R. Wischert, K. Xue, et al., ACS Catal. 4 (2014) 53–62.
[25] M. Dan-Hardi, C. Serre, T. Frot, et al., J. Am. Chem. Soc. 131 (2009) 10857.
[26] H. Wang, X.Z. Yuan, Y. Wu, et al., J. Hazard. Mater. 286 (2015) 187–194.
[27] I.D. Ivanchikova, J.S. Lee, N.V. Maksimchuk, et al., Eur. J. Inorg. Chem. 2014 (2014) 132–139.
[28] N. Maksimchuk, J.S. Lee, A. Ayupov, et al., Catalysts 9 (2019) 324.
[29] X.M. Cheng, X.Y. Dao, S.Q. Wang, et al., ACS Catal. 11 (2021) 650–658.
[30] P. Yang, Y. Huang, Z.W. Zhang, et al., Dalton Trans. 49 (2020) 10052–10057.
[31] T.L. Lu, J.P. Zou, Y.Z. Zhan, et al., ACS Catal. 8 (2018) 1287–1296.
[32] F. Bonino, A. Damin, G. Ricchiardi, et al., J. Phys. Chem. B 108 (2004) 3573–3583.
[33] Z.Q. Yang, J. Ding, J.N. Feng, et al., Appl. Organomet. Chem. 32 (2018) e4285.
[34] Z.M. Liu, Y.C. Wu, J.T. Chen, et al., Catal. Sci. Technol. 8 (2018) 1936–1944.
[35] O.A. Kholdeeva, T.A. Trubitsina, G.M. Maksimov, et al., Inorg. Chem. 44 (2005) 1635–1642.
[36] S. Bordiga, A. Damin, F. Bonino, et al., Angew. Chem. Int. Ed. 41 (2002) 4734–4737.
[37] H.X. Guo, D. Guo, Z.S. Zheng, et al., Appl. Organomet. Chem. 29 (2015) 618–623.
[38] H.H. Kim, H. Lee, D. Lee, et al., Environ. Sci. Technol. 54 (2020) 15424–15432.
[39] Z.J. Wu, K. Guo, S. Cao, et al., Nano Res. 13 (2020) 551–556.
[40] D.H. Kim, A.D. Bokare, M.S. Koo, et al., Environ. Sci. Technol. 49 (2015) 3506–3513.
[41] N. Chen, G.D. Fang, C.Y. Zhu, et al., J. Hazard. Mater. 389 (2020) 121819.
[42] G.D. Fang, Y.M. Deng, M. Huang, et al., Environ. Sci. Technol. 52 (2018) 2178–2185.
[43] Y. Liu, H. Guo, Y. Zhang, et al., Chem. Eng. J. 343 (2018) 10.
[44] C.W. Yoon, K.F. Hirsekorn, M.L. Neidig, et al., ACS Catal. 1 (2011) 1665–1678.
[45] Y. Zhou, S. Feng, X.M. Duan, et al., J. Solid State Chem. 300 (2021) 122231.
[46] G. Pan, J. Wei, M. Xu, et al., J. Hazard. Mater. 445 (2022) 130479.
[47] C.P. Gordon, H. Engler, A.S. Tragl, et al., Nature 586 (2020) 708–713.